Interaction of Recombinant Surfactant Protein D with Lipopolysaccharide: Conformation and Orientation of Bound Protein by IRRAS and Simulations[†,‡]

Lin Wang,[§] Joseph W. Brauner,[§] Guangru Mao,[§] Erika Crouch,[||] Barbara Seaton,[⊥] James Head,[⊥] Kelly Smith,[||] Carol R. Flach,*[,§] and Richard Mendelsohn[§]

Department of Chemistry, Newark College of Arts and Science, Rutgers University, Newark, New Jersey 07102, Department of Pathology and Immunology, Washington University School of Medicine, St. Louis, Missouri 63110, and Department of Physiology and Biophysics, Boston University School of Medicine, Boston, Massachusetts 02118

Received April 9, 2008; Revised Manuscript Received June 3, 2008

ABSTRACT: Effective innate host defense requires early recognition of pathogens. Surfactant protein D (SP-D), shown to play a role in host defense, binds to the lipopolysaccharide (LPS) component of Gram-negative bacterial membranes. Binding takes place via the carbohydrate recognition domain (CRD) of SP-D. Recombinant trimeric neck+CRDs (NCRD) have proven valuable in biophysical studies of specific interactions. Although X-ray crystallography has provided atomic level information on NCRD binding to carbohydrates and other ligands, molecular level information about interactions between SP-D and biological ligands under physiologically relevant conditions is lacking. Infrared reflection−absorption spectroscopy (IRRAS) provides molecular structure information from films at the air/water interface where protein adsorption to LPS monolayers serves as a model for protein−lipid interaction. In the current studies, we examine the adsorption of NCRDs to Rd_1 LPS monolayers using surface pressure measurements and IRRAS. Measurements of surface pressure, Amide I band intensities, and LPS acyl chain conformational ordering, along with the introduction of EDTA, permit discrimination of Ca^{2+}-mediated binding from nonspecific protein adsorption. The findings support the concept of specific binding between the CRD and heptoses in the core region of LPS. In addition, a novel simulation method that accurately predicts the IR Amide I contour from X-ray coordinates of NCRD SP-D is applied and coupled to quantitative IRRAS equations providing information on protein orientation. Marked differences in orientation are found when the NCRD binds to LPS compared to nonspecific adsorption. The geometry suggests that all three CRDs are simultaneously bound to LPS under conditions that support the Ca^{2+}-mediated interaction.

Surfactant proteins SP-A and SP-D[1] are members of a family of collagenous, calcium-dependent lectins (collectins) and are known to contribute to antimicrobial host defense. These two proteins bind to diverse types of carbohydrate and lipid ligands, but appear to have different specificities, modes of action, and binding propensities. For example, SP-D binds phosphatidylinositol, glucosylceramide, and the core carbohydrate region of various lipopolysachharides (LPS) found in Gram-negative bacterial cell walls, while SP-A binds to phosphatidylcholine, galactosylceramide, and the lipid A portion of LPS. Although the lung is the major site of SP-A and SP-D synthesis, the proteins have also been localized to a number of nonpulmonary sites, including the gastrointestinal and genitourinary tracts (*1, 2*). Several reviews regarding the structure and function of SP-A and SP-D have recently been published (*1, 3, 4*). The roles played by these proteins in host defense have been described in general terms; however, the molecular mechanisms of their interaction with LPS are not yet fully elucidated. SP-D, which is the focus of the current work, binds to conserved glycoconjugates on microbial surfaces and to monosaccharides such as mannose, glucose, and specific heptoses (*5, 6*).

Most native collectins are assembled as oligomers of trimeric subunits with the primary structure of individual monomers organized into four regions: an N-terminal disulfide cross-linking domain, a collagenous region, a trimeric coiled-coil neck domain (N), and a C-terminal carbohydrate recognition domain (CRD). Cooperative interactions involving the trimeric array of CRDs contribute to pattern recognition properties of SP-D thought to be important for high affinity binding to multivalent ligands and in pathogen binding. Natural SP-D predominantly assembles as dodecamers consisting of four homotrimeric subunits. However, the protein has also been isolated as trimeric subunits or higher order multimers (*7*). Quaternary structure appears important

[†] This work was supported by National Institutes of Health Grants GM 29864 (to R.M.), HL-44015, and HL-29594 (to E.C.).

[‡] Atomic coordinates for the crystal structure of this protein have been submitted to the Research Collaboratory for Structural Bioinformatics Protein Data Bank as entry 3DBZ.

* To whom correspondence should be addressed. Department of Chemistry, Rutgers University, 73 Warren Street, Newark, NJ 07102. Tel: (973)353-1330. Fax: (973) 353-1264. E-mail: flach@andromeda.rutgers.edu.

[§] Rutgers University.

[||] Washington University School of Medicine.

[⊥] Boston University School of Medicine.

[1] Abbreviations: SP-D, surfactant protein D; LPS, lipopolysaccharide; CRD, carbohydrate recognition domain; NCRD, trimeric neck+CRD; hNCRD, human NCRD; rNCRD, rat NCRD; IRRAS, infrared reflection−absorption spectroscopy; A/W, air/water; π, surface pressure; π-A, π-molecular area; initial π, π_i; L,D-heptose, L-*glycero*-α-D-*manno*-heptose.

10.1021/bi800626h CCC: $40.75
Published on Web 07/12/2008

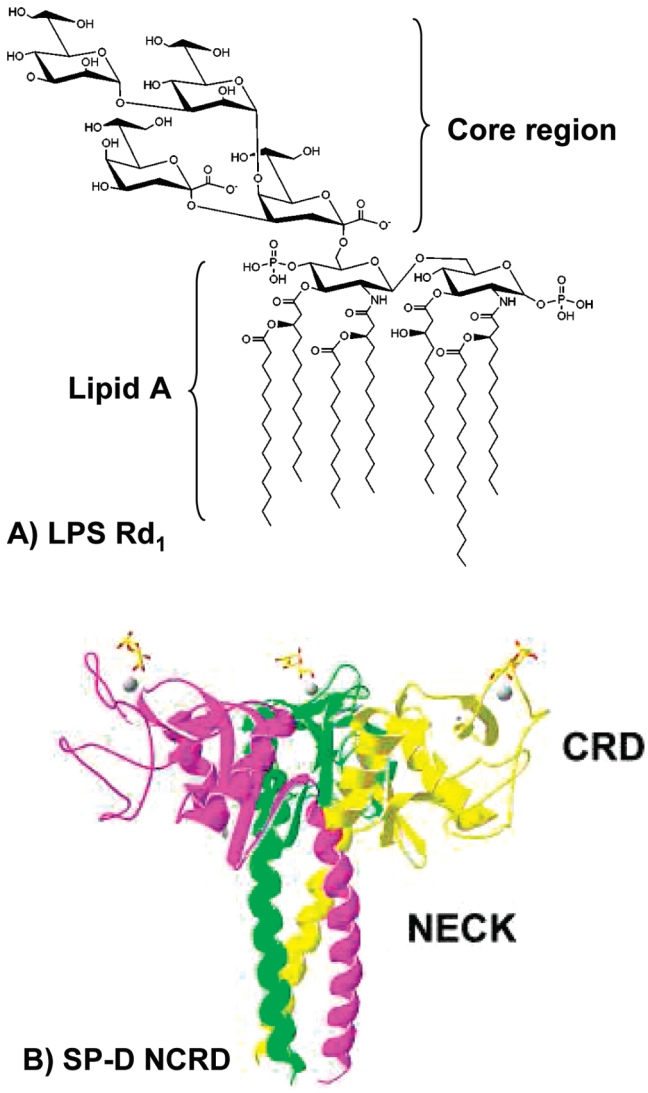

FIGURE 1: (A) Molecular structure of a generic lipopolysaccharide Rd_1 mutant with the lipid A and core regions labeled. (B) Crystal structure of trimeric SP-D NCRD complex with L,D-heptose, shown as a ribbon diagram perpendicular to the neck axis, with NCRDs in different colors. Lectin sites show calcium ions as gray spheres and L,D-heptose molecules in stick representation.

for mediating bridging interactions as four trimers stabilized by interchain disulfide bonds at their N-termini form equal length arms in an X-like structure over 100 nm long. Higher order oligomers also appear to be necessary for aggregation of some particulate ligands such as viral particles. Nevertheless, despite limited ability to promote aggregation, the trimeric form shows lectin activity with the same sugar selectivity as the full-length multimeric SP-D (*8*).

LPS molecules, essential components of Gram-negative bacterial outer membranes, are termed endotoxins due to their role in the pathogenesis of bacterial infection and septic shock (*9*). Structurally, LPS consists of a well-conserved lipid A domain and a core oligosaccharide region (see Figure 1A). In most clinical isolates, the core region terminates in a less highly conserved O-polysaccharide chain, which confers a smooth colony phenotype. Rough mutant strains do not express the O-chain and are designated Ra through Re, in order of decreasing core length. Bacterial cell walls usually contain a mixture of rough and smooth forms.

As a starting point for understanding the molecular basis of SP-D binding to bacterial surfaces, useful structural information has been acquired from recombinant trimeric fragments of human and rat SP-D (*6, 10–13*). The expressed protein, referred to as SP-D NCRD, includes the α-helical coiled-coil neck region and the carbohydrate recognition domain. Recombinant SP-D NCRD trimers generally retain the ligand binding capabilities of the full-length protein (*14*). X-ray crystallography has shown that the sugar-binding (C-lectin) site in SP-D is a shallow depression on the CRD surface (*10, 11*). A Ca^{2+} ion, coordinated to six oxygen atoms from the protein, is bound at the bottom of the pocket. Two additional coordination positions can be occupied by one or two water molecules, two cis diol oxygens from a saccharide or inositol ring with the appropriate geometry, or, as has been very recently reported, by side chain hydroxyl groups in L-glycero-α-D-manno-heptose (L,D-heptose) (*6, 12, 13*). This lectin activity has little effect on the tertiary structure of the SP-D CRD, as demonstrated by crystallographic complexes with sugars (*6, 12, 13*).

To investigate the molecular basis of collectin−LPS interaction under physiologically relevant conditions, the following technical consideration must be addressed and overcome. The size and complexity of the reactants and association products limit the applicability of high resolution crystallography and NMR approaches. Thus, although X-ray diffraction potentially provides the best structural information for studying the interactions of interest, the crystallization of either full length SP-A or SP-D is generally considered infeasible due to the length and secondary structure of the collagen-like region (73 and 177 residues, respectively). Along similar lines, the physiologically relevant states of the LPS/protein complexes (e.g., thin films, insoluble aggregates) remain poor candidates for NMR measurements.

Monolayers at the air/water (A/W) interface are likely one of the best experimental paradigms for monitoring the initial interactions that take place between the collectins and LPS molecules in the outer membrane of Gram-negative bacteria or in micelles. At the A/W interface, the hydrophobic chains of the endotoxin extend into the air, while the (polar) phosphate and sugar residues extend into the aqueous subphase as putative recognition sites for SP-D. From an experimental point of view, many useful physical properties of the system may be easily controlled, including monolayer composition, surface pressure, molecular density, and hence phase separation or domain formation. Subphase composition, temperature, and pH can also be varied. Typically, an aqueous protein solution is injected into a Langmuir trough under a preformed lipid monolayer followed by monitoring surface pressure or area changes. This protocol provides some information about the intrinsic surface activity of the protein and lipid/protein interaction; however, the elucidation of complex interactions requires a stable system and coupling the Langmuir trough measurements with other physical methods. *In situ* epifluorescence, grazing incidence X-ray diffraction, and X-ray reflectivity have recently been combined with surface pressure measurements to probe interactions between LPS-containing monolayers and SP-A or antimicrobial peptides (*15–18*).

IR and Raman spectroscopy are the only techniques that provide molecular level structural information, albeit at low resolution, from the wide variety of physical states relevant

to SP-D/endotoxin interaction. These technologies may be viewed as "vectors" which facilitate information transfer from the high resolution techniques of X-ray crystallography or NMR, where the proteins may be bound to simple sugars, to more physiologically relevant physical states (monolayers, planar bilayer films, vesicles, micelles) not amenable to high resolution structural approaches.

The current study of SP-D NCRD interaction with a purified Rd LPS (*Salmonella Minnesota* R7), utilizes infrared reflection−absorption spectroscopy (IRRAS), a technique developed in several laboratories specifically for examining monolayer films of lipids and proteins at the A/W interface (*19–22*). Along with IRRAS, standard Langmuir trough surface pressure measurements are made. To improve the quality of the structural information available from the IR spectra, a novel approach developed by the Rutgers group (*23–25*) is used to quantitatively interpret the conformation−sensitive Amide I contour (peptide bond C═O stretch, 1610−1690 cm^{-1}). The approach, discussed below, begins with the crystallographic coordinates of human SP-D NCRD either unliganded or in complex with L,D-heptose (*6*). The Amide I intensities of SP-D are then coupled to the quantitative IRRAS equations of Kuzmin and Michailov (*26, 27*) and permit us to determine the orientation of the NCRD trimer when it binds to an LPS monolayer.

EXPERIMENTAL PROCEDURES

Materials. Lipopolysaccharide from *Salmonella Minnesota* R7 (an Rd_1 mutant), Lipid A, diphosphoryl prepared from *Salmonella enterica* serotype minnesota Re 595 (Re mutant), trizma [tris(hydroxymethyl) aminomethane] hydrochloride, trizma base and sodium chloride were purchased from Sigma (St. Louis, MO). Chloroform, methanol, EDTA, and HPLC-grade water were obtained from Fisher Scientific (Pittsburgh, PA). D_2O with 99.9% isotopic enrichment was purchased from Cambridge Isotope Laboratories (Andover, MA). A generalized chemical structure of the LPS Rd_1 mutant, which terminates with L,D-heptose, is shown in Figure 1A. Heterogeneity has been observed in the acyl chain region, although generally six or seven saturated chains are present containing predominantly C14 with one C12 and one C16 chain (*28, 29*).

A trimeric, recombinant human protein lacking heterologous N-terminal tags, SP-D NCRD (hNCRD), was prepared according to Wang et al. (2008). HNCRD was purified by affinity chromatography on maltose, showing that hNCRDs used herein are competent in carbohydrate binding. A trimeric, recombinant rat SP-D NCRD (rNCRD) fusion protein was expressed and purified as previously described (*8*). A few preliminary experiments were conducted using rNCRD; all data reported herein originates from the hNCRD protein except for the rNCRD (injected at 10mN/m) data presented in Figure 3C. The final stocks of purified protein (500 μg/mL for rat and 812 μg/mL for human) were in 50 mM Tris, pH 7.5, 500 mM NaCl and 10 mM Hepes, pH 7.4, 150 mM NaCl with 5 mM $CaCl_2$, respectively.

Crystallographic Analysis of Protein Constructs. X-ray crystallographic coordinates used in these studies were obtained from 1.8 Å resolution crystal structures of hNCRD SP-D, either in complex with L,D-heptose (PDB code 2RIB; (*6*)) or with no sugar present (PDB code 3DBZ; J. Head and B. Seaton, unpublished work). Crystals were prepared as described previously from PEG solutions containing calcium chloride (*12*). The heptose complex (Figure 1B) was obtained through a crystal soaking protocol described previously (*6*). Atomic coordinates sets used for calculations consisted of the SP-D trimers (backbone atoms only) with no solvent or ions included.

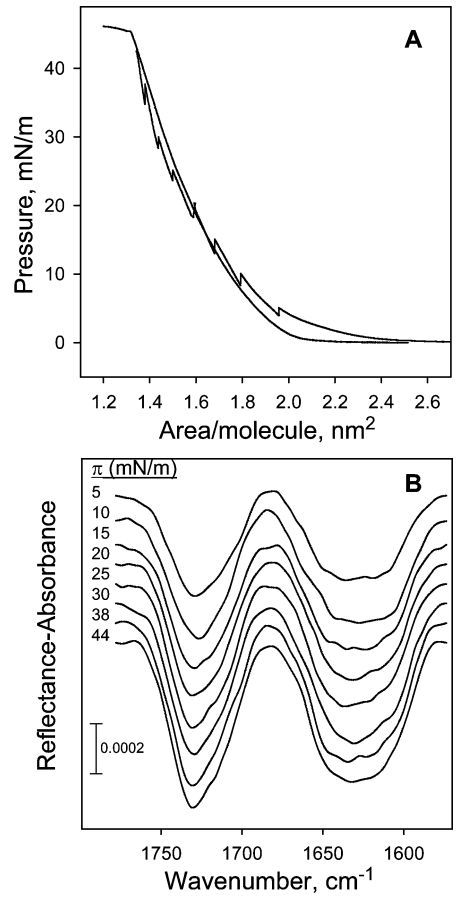

FIGURE 2: (A) Surface pressure−molecular area isotherms of Rd_1 LPS monolayers spread on a Tris buffer (pH 6.9) and 150 mM NaCl subphase containing 4 mM Ca^{2+}. The isotherms were acquired on two different troughs using continuous (smooth curve) versus intermittent (jagged isotherm) compression to demonstrate the stability of the Rd_1 monolayer. Intermittent compression is required when collecting IRRAS spectra as shown in (B) for the Rd_1 monolayer at increasing surface pressure (top to bottom) over the 1780−1575 cm^{-1} spectral region.

Sample Preparation and Lipid Isotherm Acquisition. Solutions of the Rd_1 LPS were prepared in chloroform/methanol (10/1, v/v) at ~1 mg/mL concentration by gentle warming. A Nima 611 LB trough (Nima Technology, Inc., Coventry, England; maximum surface area approximately 600 cm^2) with a model PS4 surface pressure sensor was used for the acquisition of LPS monolayer surface pressure-molecular area (π-A) isotherms. Typically, 25 μL of the lipid solution was spread on a 150 mM NaCl, 5 mM Tris (pH 6.9), and 4 mM $CaCl_2$ subphase at 21.5 ± 0.5 °C at large molecular areas. Following a 30 min equilibration period to allow for solvent evaporation and film relaxation, monolayers were compressed at 15 cm^2/min while isotherms were recorded.

IRRAS Measurements of LPS and LPS/Protein Films. IRRAS spectra were acquired with a Bruker Instruments Equinox 55 spectrometer equipped with an external variable

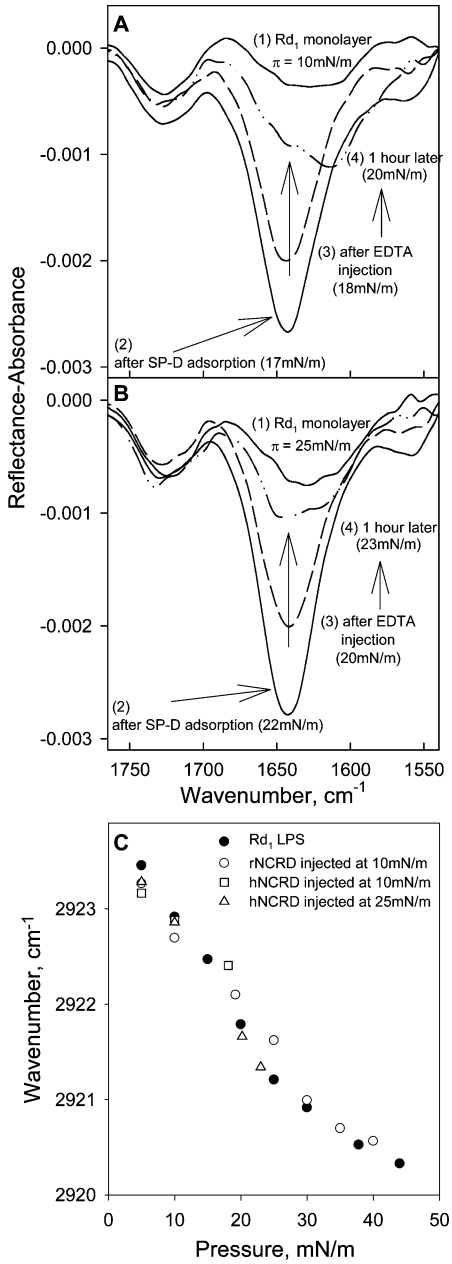

FIGURE 3: IRRAS spectra (1765−1540 cm^{-1}) of SP-D NCRD adsorption to Rd_1 monolayers initially compressed to surface pressures of (A) 10 mN/m and (B) 25 mN/m. Spectra were acquired (1) prior to and (2) following protein subphase injection and pressure equilibration. Subsequently, an EDTA solution was injected into the subphase, and spectra were acquired after (3) 10 min and (4) 1 h. (C) The surface pressure dependence of Rd_1 LPS acyl chain conformational ordering monitored by asymmetric methylene stretching frequencies. Separate experiments were conducted in the absence and presence of adsorbed rat or human SP-D NCRD proteins when the LPS monolayers were initially compressed to 10 or 25 mN/m as noted.

angle reflectance accessory, the XA511. The accessory is coupled to a custom-designed Langmuir trough (maximum surface area of 86 cm^2) constructed by Nima Technology Ltd. (Coventry, England) with a model PS4 surface pressure sensor. IRRAS spectra are acquired with a wire grid polarizer mounted in the optical path. Computer-driven stepper motors rotate the mirrors to obtain the desired angle of incidence. The reflected light is directed onto a narrow band mercury/cadmium/telluride (MCT) detector. The entire experimental setup is enclosed and purged to control the relative humidity levels. Additional trough and instrument details have been previously reported (*30*).

Interferograms were collected with the use of a sample shuttle program to compensate for the residual water vapor. For each spectrum, a total of 2048 scans were acquired at ~8 cm^{-1} resolution, in 4 blocks of 512 scans each, coadded, apodized with a Blackman-Harris-3-term function, and fast Fourier transformed with one level of zero-filling to produce spectral data encoded at ~4 cm^{-1} intervals. IRRAS spectra are reported as $-\log (R/R_o)$, where R is the intensity of light reflected from the film-covered surface and R_o is the intensity of light reflected from the background surface.

IRRAS experiments were conducted as follows. Aliquots of ~10 μL of LPS solution were spread dropwise on a D_2O-based subphase (same composition as described above) and 45 min were allowed for equilibration. The initial surface pressure for all experiments was 0 mN/m. Spectra were collected during intermittent compression while π-A isotherms were recorded. A barrier speed of 1 cm^2/min was used. The barrier was stopped at particular surface pressure values and a relaxation period of 5 min was allowed before spectral acquisition. Unless otherwise noted, spectra were collected using s-polarized light at a 50° angle of incidence. For studies of SP-D NCRD adsorption, when the desired surface pressure (10 or 25 mN/m) was reached, 60 μL of the protein solution (~0.8 mg/mL) was injected beneath the preformed LPS monolayer. When the surface pressure had stabilized (15−30 min), spectra of the lipid/protein film were acquired. For orientation studies, spectra were acquired at various angles of incidence (typically from 34 to 48° in 2° increments) using s- and p-polarized radiation (*30*). Within the IRRAS spectral acquisition time, there was no indication of protein diffusion to the reference side of the trough. Subsequently, in particular experiments, 1.5 mL of EDTA solution (~0.2M) was injected into the subphase to a final concentration of ~5 mM and spectra were collected as a function of time. Finally, additional control experiments were conducted with lower concentrations of EDTA being injected into the subphase (final concentration 0.006−0.5 mM).

IRRAS Data Analysis. Data analysis was performed using Grams/32 software (Galactic Industries Corp., Salem, NH, USA) to determine peak intensity at particular frequencies within the Amide I contour after linear baseline correction. Peak positions for the methylene asymmetric stretching mode were determined with a center-of-gravity algorithm written by D. Moffatt and provided by the National Research Council of Canada.

Simulations of the IRRAS Amide I Band and the Determination of Trimer Orientation. Reflectance−absorbance Amide I bands of the trimeric form of SP-D adsorbed at the A/W interface were obtained for a series of angles of incidence using s- and p-polarized light. By simulating the Amide I band as described below we are able to discern the tilt of the trimer's symmetry axis with respect to the water surface.

At the outset, it is noted that our simulations require the crystallographic coordinates of the peptide bonds. Our approach regards the Amide I contour as resulting from a collection of interacting oscillators (one per peptide bond). The interactions between the oscillators are calculated from geometry-sensitive formulas suggested by elementary physics. A single set of parameters based on the above interactions

was previously used to simulate, with excellent accuracy, the Amide I contour of ~15 proteins comprising a variety of secondary structures (*24*).

The optical theory of Kuzmin (*26, 27*) was used to calculate the reflectance−absorbance of the Amide I mode for the adsorbed protein film as previously discussed in detail (*31*). The calculation requires the laboratory frame Cartesian components of the index of refraction and the extinction coefficient of the protein film. The extinction coefficient of a given vibrational mode depends on the square of the resultant transition dipole moment for that mode. Beginning with atomic coordinates from a three-dimensional protein structure, our Amide I band simulation method (*24*) permits us to obtain the Cartesian components of the transition dipole moments for each mode of vibration in the molecular frame. These then can be converted into the laboratory frame components by an Euler angle transformation based on an assumed geometric relation between the molecule and the water surface.

The trimeric form of hNCRD (*6, 12*) has 450 peptide bonds. In our coupled oscillator model each trimer therefore has 450 Amide I modes of vibration. The contribution of each peptide group to each of these modes is given by the inverse L matrix as found by our Amide I band simulation algorithm. This permits a weighted sum of transition dipole components in the molecular frame to be calculated for each mode.

The extinction coefficient and the index of refraction are related as the real and imaginary parts of the square root of the complex dielectric constant seen by the light propagating through the surface layer. The equations in Becker (*32*) for an elastically bound electron were used to model n and k. In addition, a 30% Gaussian−70% Lorentzian band shape was used to broaden the extinction coefficient lines. The common factors in the Cartesian components of n and k were the laboratory frame values of the extinction coefficient components as computed from the square of the laboratory frame transition dipole components. These values were adjusted by a common strength factor to make the simulated band fit the experimental IRRAS band. The central value for the refractive index of the film was taken to be 1.41. The final values for n and k are given by the summation of 450 terms, one for each normal mode of vibration for the coupled oscillator system.

The Cartesian components of the transition dipoles in the molecular frame can be converted into components in the laboratory frame by the Euler angle transformation matrix as found in appendix I of Wilson, Decius, and Cross (*33*). The Euler angle transformation had also been used prior to the Amide I simulation to make the symmetry axis of the trimer parallel to the molecular *z*-axis. Then the polar angle, theta, between the molecular *z*-axis and the laboratory Z-axis perpendicular to the water surface gives the tilt of the trimer with respect to the water surface. The other two Euler angles, phi and chi, were kept constant at 45°.

RESULTS

LPS Monolayers. Overlaid π-A isotherms of Rd_1 LPS monolayers (shown in Figure 2A), used in the current experiments as a model for the outer leaflet of the outer membrane of Gram-negative bacteria or LPS micelles, demonstrate the relative stability of the lipid films. The isotherms were acquired using two different troughs and very different methods of compression. In general, they show that Rd_1 LPS forms a somewhat expanded monolayer, stable, under continuous compression (smooth curve), up to pressure values of at least 40 mN/m. The overall similarity between the two suggests that the relaxation processes occurring during intermittent compression (jagged isotherm), necessary for acquiring IRRAS spectra, do not destabilize the film during the time required to complete this experiment, approximately 1−2 h. High quality IRRAS spectra (1800−1575 cm^{-1} region) acquired during intermittent monolayer compression are shown in Figure 2B. The ester carbonyl band is observed at ~1735 cm^{-1} along with a broad Amide I and carboxylate feature (1600−1650 cm^{-1}). Two of the corresponding functional groups (ester carbonyl and amide group) are found in the lipid A portion of LPS and the carboxylates are found in the core region (see Figure 1A). Band intensity increases with pressure are consistent with film stability; band shape changes are minimal indicating that the environment (e.g., hydration) of these groups stays essentially the same over the 5−44 mN/m pressure range sampled.

LPS/SP-D NCRD IRRAS Experiments: Binding Studies. Investigations of binding between the SP-D hNCRD trimer and Rd_1 LPS were conducted by injecting a protein solution underneath a preformed LPS monolayer compressed to specific initial surface pressure values (π_i) on a Ca^{2+}-containing subphase. Experiments were conducted at π_i = 10 and 25 mN/m. One reason the initial pressure of 25 mN/m was selected is because it falls within the range reported for biological membranes (*34, 35*). In each experiment, IRRAS spectra were acquired before and after protein injection allowing time for equilibration of surface pressure (Figure 3A and B). A small decrease in pressure was observed for both lipid films during the equilibration period prior to protein injection. Surface pressure decreased to ~8 mN/m for π_i = 10 mN/m and to ~20 mN/m for π_i = 25 mN/m. Following the adsorption of protein and data acquisition, an EDTA solution was injected into the subphase to evaluate the Ca^{2+}-dependence of the LPS/NCRD interaction, as well as the effects of chelation on the LPS monolayer.

When the LPS monolayer was initially compressed to a pressure value of 10 mN/m, a rapid increase in pressure was observed upon protein injection which stabilized at ~17 mN/m after 10 min. Representative IRRAS spectra over the 1770−1540 cm^{-1} range are shown in Figure 3A before and after protein adsorption, along with two spectra obtained following the injection of an EDTA solution into the subphase. IRRAS spectra from the π_i = 25 mN/m experiment (π = 20 mN/m upon film relaxation), are presented in Figure 3B. In this experiment, a small, rapid increase in pressure from 20 to 22 mN/m was observed after SP-D hNCRD was injected into the subphase.

The spectrum labeled (2) in each panel of Figure 3 was acquired following protein injection and pressure equilibration. IRRAS intensity in the 1600−1650 cm^{-1} region from LPS monolayers (arising from the carboxylate and Amide I modes of LPS) is assumed to remain constant after the SP-D injection, as is observed for the LPS ester carbonyl band (~1735 cm^{-1}). Upon protein injection, a significant increase in Amide I intensity relative to the LPS ester carbonyl band (difference between spectra labeled (1) and (2) in each panel)

is evident for both high and low pressure experiments. Amide I band position and shape are very similar in both cases indicating that the secondary and tertiary structures of hNCRD are essentially the same regardless of lipid packing (over the pressure range studied). In addition, a carboxylate asymmetric stretching band at ~1570 cm^{-1}, thought to arise from the CRD region of the protein, is present in the ternary system (LPS/SP-D/Ca^{2+}, see spectrum labeled (2) in Figure 3A and B). The protein carboxylate band was previously shown to be a specific marker for a similar Ca^{2+}-dependent interaction between a phospholipid and the lung surfactant collectin protein SP-A in bulk phases (*36*). In the current set of experiments, the appearance of the carboxylate band (1570 cm^{-1}) of SP-D appears to be dependent on the presence of Ca^{2+} and independent of the presence of lipid (not shown).

Evidence of Ca^{2+}-dependent LPS-NCRD binding was observed when an EDTA solution was subsequently injected into the subphase. Spectra acquired after the addition of EDTA (10 min (3) and 1 h (4) in Figure 3A and B) display a significant decrease in Amide I intensity with time. Not long after the EDTA injection (~10 min), the intensity of the protein carboxylate band is reduced to the noise level, whereas the Amide I band contour, although reduced in intensity, maintains essentially the same position and shape (compare spectra labeled (2) and (3) in Figure 3A and B). One hour after addition of EDTA, the intensity in the Amide I region is significantly reduced and the contour changes dramatically, most likely reflecting predominant contributions from LPS and EDTA with little residual protein remaining at the interface. Throughout the experiment, the LPS ester carbonyl band (~1735 cm^{-1}) appears unchanged by the EDTA injection. As a control, IRRAS spectra were acquired after an EDTA solution (final subphase concentration ~5 mM) was injected under an Rd_1 LPS monolayer initially compressed to ~10 mN/m. After approximately 40 min, a moderate surface pressure increase to ~12 mN/m was observed along with an additional band (shoulder) at ~1615 cm^{-1}, most likely due to the carboxylate asymmetric stretch of EDTA (not shown). The time scale for the appearance of 1615 cm^{-1} shoulder is approximately the same for experiments run in the presence and absence of protein, most likely reflecting the low surface activity of EDTA. In an additional control experiment designed to examine the effects of EDTA on protein structure, a less concentrated EDTA solution (final concentration ~0.006 mM) was injected into a Ca^{2+}-free subphase after adsorption of the NCRD to a lipid-free A/W interface. The Amide I band shape and position remained basically the same as displayed in Figure 3 over 6 h (not shown). We note that Ca^{2+}-free crystal structures are not available. Therefore small spectral changes in the Amide I contour cannot be quantitatively interpreted. The concentration of EDTA in the second control experiment was more than sufficient to bind the Ca^{2+} introduced with the protein injection but low enough so that it is either below our detection limit or did not appreciably adsorb to the A/W interface as is indicated by the lack of a band at 1615 cm^{-1} and the lack of a pressure increase.

Surface pressure-induced conformational ordering in the acyl chains of an Rd_1 LPS monolayer is indicated by the shift to lower frequency in the asymmetric methylene stretching mode as displayed in Figure 3C. Only a slight

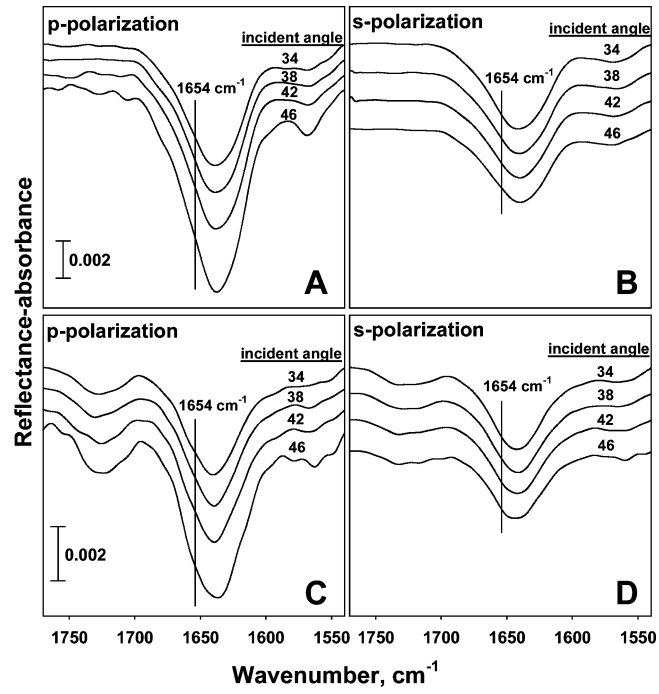

FIGURE 4: IRRAS spectra (1765−1540 cm^{-1} region) acquired using s- and p-polarized radiation for hNCRD SP-D adsorbed to (A) and (B) a clean A/W interface and to (C) and (D) an Rd_1 LPS monolayer initially compressed to 10 mN/m at various angles of incidence. Band intensity at the 1654 cm^{-1} position, noted by the vertical line drawn on the Amide I band, is used to determine the orientation of the protein at the interface.

deviation, in the 15−25 mN/m surface pressure range, is observed in the frequency versus pressure plots following the introduction of either rat or human SP-D NCRD under the lipid monolayers. At pressure values greater than 25 mN/m, further frequency decreases are essentially independent of the presence of the protein suggesting that SP-D NCRD binding to the core oligosaccharide does not greatly perturb the pressure-induced packing of the LPS acyl chains.

LPS/SP-D NCRD IRRAS Experiments: Orientation Studies. The nature of the A/W interface together with the physical and chemical characteristics of the sample components imparts a specific geometry to the systems under study. The resulting organization can be exploited to obtain information about the orientation of particular molecular regions upon protein/lipid binding by acquiring IRRAS spectra using polarized light at a variety of angles of incidence. Measurements were again conducted at initial pressure values 10 and 25 mN/m. Although, based on the analysis below, it might have been useful to carry out measurements at higher initial pressure values (35−40 mN/m), this was not feasible due to the following. Polarized IRRAS measurements over a range of incident angles require film stability (at a specific pressure value) for 5−6 h. Whereas, the Rd_1 monolayer is stable enough to acquire the spectra shown in Figure 2B at $\pi \geq 30$ mN/m (equilibration and acquisition time requires ~15 min/spectrum), film stability deteriorates over the longer time scales (at $\pi \geq 30$ mN/m) required for orientation studies.

IRRAS spectra acquired after hNCRD SP-D was injected into the subphase in the presence and absence of an Rd_1 monolayer in the 1540−1770 cm^{-1} region are shown in Figure 4. The spectra shown in Figure 4, A and B, were acquired after the protein adsorbed to a clean A/W interface

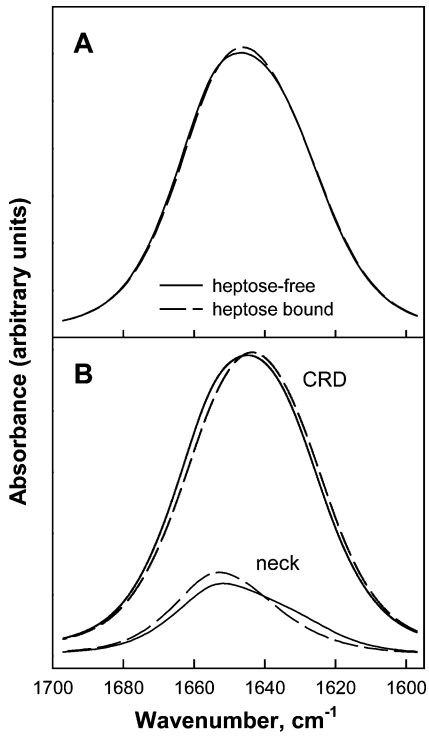

FIGURE 5: (A) Simulated Amide I contours for hNCRD SP-D calculated from the coordinates of the crystallographic complexes with (dashed line) and without (solid line) bound L,D-heptose. (B) Amide I sub-bands corresponding to contributions from peptide bonds in the neck and the CRD regions of the protein using the same designations as in (A).

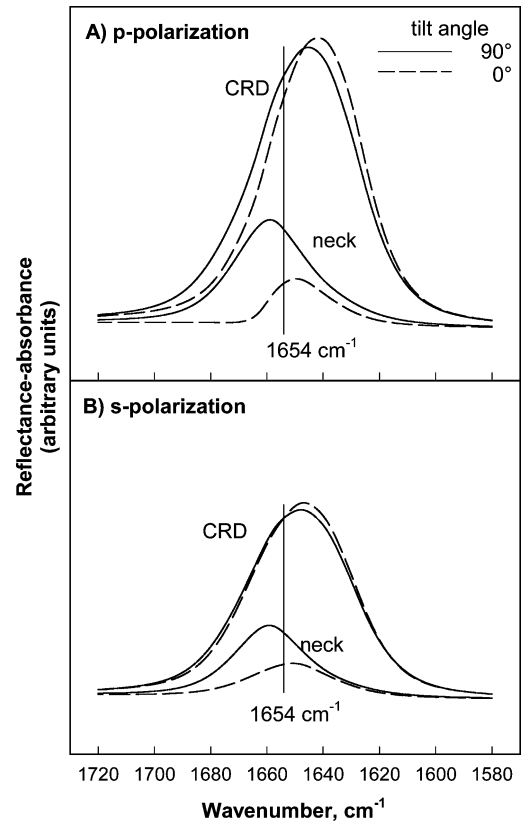

FIGURE 6: Simulated IRRAS Amide I sub-bands (inverted) for the neck and CRD regions of hNCRD SP-D based on the X-ray coordinates of the protein with bound L,D-heptose. The calculation was performed using an incident angle of 36° for (A) p-polarization and (B) s-polarization with the tilt angle of the neck axis aligned at 90° (solid line) and 0° (dashed line) with respect to the normal to the A/W interface. A vertical line is drawn at 1654 cm^{-1} to highlight the sensitivity of the intensity in the neck sub-band to orientation.

whereas the spectra shown in Figure 4, C and D, were acquired in the presence of an Rd_1 LPS monolayer initially compressed to 10 mN/m. Similar spectra were obtained for the $\pi_i = 25$ mN/m experiment (not shown). For all data sets, the Amide I band intensity (centered at ~1640 cm^{-1}) varies with angle of incidence for both s- and p-polarization in a predictable way (*31*). In particular, a slight decrease in the Amide I band intensity using s-polarization and a significant increase in intensity using p-polarization is observed as the incident angle increases. Differences in the degree of intensity variation in the presence compared to the absence of lipid are noted, especially for the spectra acquired using p-polarization.

In order to extract orientation information from IRRAS spectra of proteins, a region of secondary structure with a well-defined molecular axis is required. Considering a monomer in the protein under study, the uninterrupted coiled-coil neck region meets the necessary requirements while the CRD, containing short segments comprised of various secondary structures, does not. The resultant transition dipole moment change in the CRD for all the modes essentially cancels out. In the following calculations, the first step was to align the symmetry axis of the trimer with the molecular *z*-axis as discussed in the Simulation section. The tilt angle of the trimer (angle between the molecular *z*-axis and the normal to the water surface) was determined using the following approach.

The overall Amide I band contour was simulated for the trimeric SP-D fragment as described in the Experimental section (*24, 25*). Simulated spectra derived from the crystal structure coordinates of human, trimeric NCRD SP-D, free and with bound L,D-heptose are displayed in Figure 5A. Both structures contain three bound calcium ions per CRD. As expected from a comparison of the two crystal structures, the two simulated Amide I bands are quite similar. One benefit of the simulations is the ability to extract the spectral contribution from any region of the protein as is shown in Figure 5B which displays simulated Amide I sub-bands from the neck and CRD regions.

Simulated Amide I contours were transformed into the IRRAS framework as described in the Simulation section. IRRAS Amide I sub-bands (inverted) simulated for the neck and CRD regions of the heptose-bound structure are displayed in Figure 6 and are essentially the same as bands generated for the unliganded structure using the same parameters (not shown). Simulations were conducted using an angle of incidence of 36° and tilt angles of 0° and 90° to demonstrate the sensitivity of the neck region to orientation. It is evident that the CRD contour is relatively insensitive to orientation, because the overlaid bands for the two tilt angles do not differ significantly, especially for s-polarized radiation. In contrast, the simulated sub-bands arising from the neck oscillators vary significantly for both s- and p-polarization when comparing the two tilt angles. In an attempt to exploit this sensitivity, the band intensity in the simulated Amide I contour at 1654 cm^{-1} was obtained for s- and p-polarization over a range of angles of incidence at various neck tilt angles. Similar intensity measurements were made at 1654 cm^{-1} on the experimental data as marked by

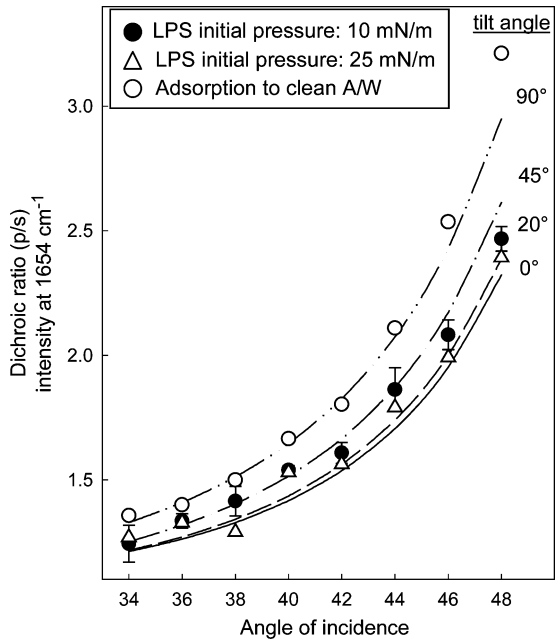

FIGURE 7: Determination of NCRD SP-D orientation at the A/W interface in the presence and absence of Rd_1 monolayers by comparing the dichroic ratios calculated from simulated Amide I band intensities at 1654 cm^{-1} over a range of incident angles (lines, at particular neck axis tilt angles as noted) with experimentally measured dichroic ratios (symbols: (○) clean A/W interface; (●) Rd_1 monolayer initially compressed to 10 mN/m and (△) to 25 mN/m). The mean and standard deviation for four separate experiments are shown for Rd_1 monolayers compressed to 10 mN/m, and averages for two experiments are shown for the remaining two data sets.

the vertical lines in Figure 4. Dichroic ratios (p/s intensity) were calculated from the simulated and experimental Amide I band intensities to determine the orientation of the molecular axis, i.e. the tilt angle of the neck region with regard to the normal to the A/W interface.

Experimental dichroic ratio values measured using three different sets of conditions are plotted over a range of incident angles along with curves generated from simulated Amide I band intensities calculated at various tilt angles (Figure 7). The experimental values were obtained from SP-D hNCRD adsorption to a clean A/W interface and to Rd_1 monolayers initially compressed to surface pressures of 10 and 25 mN/m. The simulated curves are based on the coordinates of the L,D-heptose-bound protein structure. The best fit to the experimental data in the absence of an LPS monolayer was found for the simulations where the molecular axis was essentially parallel to the A/W interface, i.e., a tilt angle close to 90°. By contrast in the presence of LPS monolayers, the best fit to the experimental dichroic ratio values for the LPS $\pi_i = 10$ mN/m experiment yields a tilt angle range of 20−45°, and a tilt angle closer to 20° for the LPS $\pi_i = 25$ mN/m experiment. As anticipated, a 0−20° tilt angle would likely allow for the simultaneous binding of all three CRDs with heptose groups in the core region of LPS molecules.

DISCUSSION

In the present work, we describe the use of IRRAS to study specific molecular interactions associated with SP-D NCRD adsorption to LPS monolayers. One unique feature of the current study is our ability to obtain structural information about SP-D binding to a biological ligand under physiologically relevant conditions. In the following discussion, the results of IRRAS experiments regarding the Ca^{2+}-dependence of the interaction, nonspecific protein adsorption to the A/W interface versus specific ligand binding, and the orientation of the hNCRD trimer will be discussed in the context of these data, providing support for specific binding between the CRD of SP-D and the core region of the Rd_1 monolayer.

SP-D NCRD Adsorption to the Rd_1 LPS Monolayer. Ca^{2+}-dependence is clearly evident in the binding of the SP-D NCRD to LPS monolayers. Protein desorption from such monolayers upon the introduction of EDTA into the subphase is consistent with Ca^{2+}-mediated binding between the CRD and LPS. Control experiments along with spectra shown in Figure 3 corroborate that EDTA, as introduced in the current experiments, has at most a small effect on the measured IR contours for either Rd_1 or NCRD. EDTA acts primarily as a Ca^{2+} chelating agent. Based on the results presented herein, along with recent crystallographic studies and inhibition assays investigating the lectin activity of hNCRD, we suggest that binding takes place between the CRD and L,D-heptose in the core region of Rd_1 LPS (*6*).

The increase in pressure (∼7 mN/m for hNCRD, Figure 3A and 10 mN/m for rat NCRD, not shown) observed after protein injection for the $\pi_i = 10$ mN/m experiments likely reflects the intrinsic surface activity of the protein as it adsorbs to the A/W interface. This adsorption reduces the surface area available to the lipid molecules and results in acyl chain ordering as is evident in the plots of the methylene asymmetric stretching frequencies (Figure 3C, $\pi_i = 10$ mN/m). For both experiments ($\pi_i = 10$ and 25 mN/m), the pressure induced acyl chain ordering is, to a large extent, independent of the presence of protein consistent with the lack of a specific (hydrophobic) interaction between the NCRD and the LPS acyl chains.

The combination of surface pressure and IRRAS measurements allows us to differentiate between nonspecific adsorption to the A/W interface or to the LPS monolayer and specific binding of protein to the LPS monolayer. Prior studies (*37*) have shown that surface pressure measurements, which probe penetration into the lipid layer, are insensitive to adsorption below the lipid monolayer. In the current set of experiments, surface pressure measurements are also shown to be insensitive to specific Ca^{2+}-mediated binding taking place in the vicinity of the LPS heptose groups and the subphase, i.e., below the lipid monolayer. Support for this claim comes from the high pressure experiment ($\pi_i =$ 25mN/m) where the intensity of the Amide I band is significantly larger than expected for a 2 mN/m pressure increase. The small pressure increase indicates that relatively small amounts of protein adsorb to the A/W interface. Whereas the intensity of the Amide I band alone may be indicative of nonspecific adsorption to the monolayer and/or specific binding, the Ca^{2+}-dependence discussed above is only consistent with specific binding.

The following comparison reinforces the concept that the binding interaction between SP-D and LPS involves the lipopolysaccharide core domain rather than the lipid portion of the molecule. In separate experiments, hNCRD was injected beneath diphosphoryl lipid A monolayers initially compressed to pressure values of either 10 or 30 mN/m. Lipid

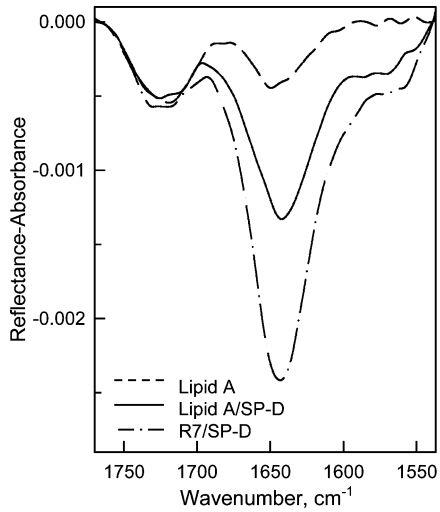

FIGURE 8: Overlaid IRRAS spectra (1765−1540 cm^{-1}) comparing hNCRD SP-D adsorption to Lipid A and Rd_1 monolayers (as noted) initially compressed to a surface pressure of 10 mN/m after equilibration of pressure to ~17 mN/m for both experiments. A spectrum of Lipid A at π = 10mN/m prior to protein injection is also shown.

A lacks the specific carbohydrate moieties (see Figure 1A) implicated in SP-D binding as suggested by binding assays and X-ray crystallography (*6, 12, 13*), but consists of essentially the same lipid acyl chain distribution as the Rd_1 LPS. Amide I band intensity was significantly lower following protein injection under Lipid A compared to Rd_1 monolayers for both initial conditions (low and high pressure). IRRAS spectra (1765−1540 cm^{-1}) are overlaid in Figure 8 following hNCRD injection under Lipid A versus Rd_1 monolayers initially compressed to 10mN/m. An IRRAS spectrum of the Lipid A monolayer prior to protein introduction is also included in the figure. Whereas the pressure increase upon protein adsorption is nearly identical for the two lipids (final pressure of 16−17 mN/m), the Amide I intensity is not. We infer that the Amide I intensity for the Lipid A, low pressure experiment arises mainly from nonspecific protein adsorption to the A/W interface. The majority of the additional band intensity for the corresponding Rd_1 experiment is likely due to specific binding interactions between the core region of Rd_1 and the CRD of SP-D. In addition, the Amide I band intensity is significantly smaller (peak height <0.001 RA) after protein is injected under a Lipid A monolayer compressed to 30 mN/m (not shown) where adsorption to the A/W interface would be minimal. Based on all the adsorption measurements, we infer that the equilibrium pressure of the hNCRD lies between 22−30 mN/m. Consistent with the above observations, previous studies report minimal binding between hNCRD and Re-LPS or Kdo (3-deoxy-α-D-manno-oct-2-ulosonic acid) (*6*). This comparison illustrates the utility of the IRRAS protocol to serve as a qualitative binding assay while providing information regarding the specificity of the interaction.

In an earlier report, Taneva et al. (*38*) investigated the surface activity of full-length recombinant rat SP-D by measuring surface pressure changes in the presence and absence of phospholipid monolayers. To the best of our knowledge, this is the only other published study regarding the interaction of SP-D with lipid monolayers. The authors (*38*) are careful to note that there may be inadequacies in interpretations of experiments involving surface pressure changes in the absence of additional corroborating measurements. Taneva et al. suggest that hydrophobic forces drive the lipid/protein interaction independent of the lipid headgroup, implying a significant role for the lipid acyl chains. However, in their study, the presence of calcium in the subphase attenuated the surface activity of the protein and its ability to generate surface pressure changes upon adsorption to lipid monolayers. We suggest that a portion of the pressure increase observed by Taneva et al., arises from nonspecific adsorption of the protein to the hydrophobic A/W interface, possibly explaining part of the lipid headgroup independence. Of course, we cannot rule out the possibility that the full-length protein may have a stronger interaction with lipid acyl chains than the NCRD used herein. Nevertheless, our results suggest that interactions are dominated by Ca^{2+}-dependent binding with the core region of LPS.

Protein Molecular Orientation. To understand the correlation between the Amide I spectral contour and the three-dimensional protein structure in more detail, we have developed a method (*24, 25*) that permits us to predict the Amide I spectrum from the crystal structure of hNCRD. Coupling the Amide I contour simulations with the quantitative IRRAS equations allows us to ascertain the orientation of the adsorbed protein relative to the monolayer surface. As is evident in the simulated dichroic ratio curves plotted in Figure 7, our ability to distinguish between tilt angles decreases as tilt angle values decrease (simulated curves are closer together at lower tilt angles). In addition, the simulated curves also tend to coincide as the angle of incidence decreases. Therefore, more weight is placed on finding the best fit to the experimental data for the larger angles of incidence as plotted in Figure 7.

Following protein adsorption for the π_i = 10 mN/m experiment, the dichroic ratio values yield a neck tilt angle range of 20−45°. The tilt angle appears to be on the low end of this range (~20°) for the π_i = 25 mN/m experiment. We suggest that the broadened range of tilt angles at the lower pressure reflects the presence of two populations of adsorbed hNCRD, each population defined by its orientation. It is reasonable to assume, for example, that one pool of protein molecules exists with a 0−20° neck tilt angle and reflects the SP-D population associated with specific ligand interactions, and a second pool adsorbed to the A/W interface with a 90° tilt. This heterogeneity is observed when the lipid was initially compressed to 10 mN/m, but diminishes at higher pressures. A linear combination of these two populations would produce the measured dichroic ratio values as plotted and yields the 20−45° tilt angle range. An analogous procedure was previously utilized to describe the orientation of helical pulmonary surfactant protein C in monolayer environments (*39*).

The coupling of the overall Amide I contour simulations with quantitative IRRAS tilt determinations leads to reasonable results (0−20° neck tilt) for binding to LPS monolayers. This geometry suggests that all three CRDs contact the monolayer and that the coiled neck region extends into the subphase approximately normal to the A/W interface. In contrast, in the absence of LPS, the tilt angle of the neck region of hNCRD was approximately parallel to the water surface (90°). With this orientation, lateral CRD surfaces

would contact the interface, precluding involvement of all three ligand-binding surfaces (*6, 10–13*).

In summary, the IRRAS findings extend recent studies showing that SP-D can bind to Rd-LPS (*6*). In particular, the current findings demonstrate specific binding in the context of a defined lipid layer. Poor binding to Lipid A monolayers is consistent with preferential binding to the heptose-rich inner core oligoscaccharide region. Specific binding of hNCRD to Rd_1 LPS monolayers is Ca^{2+}-dependent and consistent with a molecular orientation that places the trimer axis close to perpendicular to the monolayer plane. In this orientation, all three CRD subunits are positioned to form specific interactions between the lectin sites and LPS core saccharides. Without ligand, the binding interactions that promote the perpendicular orientation are absent, as reflected by the vastly different tilt angle; hydrophobic or other forces become key in orienting the molecule adsorbed at the water surface. The findings are relevant to interactions between pulmonary surfactant and glycoconjugates present in micelles or associated with microbial cell walls and viral envelopes.

REFERENCES

1. Wright, J. R. (2005) Immunoregulatory functions of surfactant proteins. *Nat. Rev. Immunol. 5*, 58–68.
2. Crouch, E. C. (2000) Surfactant protein-D and pulmonary host defense. *Respir. Res. 1*, 93–108.
3. Sano, H., and Kuroki, Y. (2005) The lung collectins, SP-A and SP-D, modulate pulmonary innate immunity. *Mol. Immunol. 42*, 279–287.
4. Kishore, U., Greenhough, T. J., Waters, P., Shrive, A. K., Ghai, R., Kamran, M. F., Bernal, A. L., Reid, K. B. M., Madan, T., and Chakraborty, T. (2006) Surfactant proteins SP-A and SP-D: Structure, function and receptors. *Mol. Immunol. 43*, 1293–1315.
5. Crouch, E., and Wright, J. R. (2001) Surfactant proteins A and D and pulmonary host defense. *Annu. Rev. Physiol. 63*, 521–554.
6. Wang, H., Head, J., Kosma, P., Brade, H., Muller-Loennies, S., Sheikh, S., McDonald, B., Smith, K., Cafarella, T., Seaton, B., and Crouch, E. (2008) Recognition of heptoses and the inner core of bacterial lipopolysaccharides by surfactant protein D. *Biochemistry 47*, 710–720.
7. Crouch, E., Hartshorn, K., and Ofek, I. (2000) Collectins and pulmonary innate immunity. *Immunol. Rev. 173*, 52–65.
8. Crouch, E. C., Smith, K., McDonald, B., Briner, D., Linders, B., McDonald, J., Holmskov, U., Head, J., and Hartshorn, K. (2006) Species differences in the carbohydrate binding preferences of surfactant protein D. *Am. J. Respir. Cell Mol. Biol. 35*, 84–94.
9. Brandenburg, K., and Wiese, A. (2004) Endotoxins: Relationships between structure, function, and activity. *Curr. Top. Med. Chem. 4*, 1127–1146.
10. Hakansson, S., Lim, N. K., Hoppe, H.-J., and Reid, K. B. M. (1999) Crystal structure of the trimeric α-helical coiled-coil and the three lectin domains of human lung surfactant protein D. *Structure 7*, 255–264.
11. Shrive, A. K., Tharia, H. A., Strong, P., Kishore, U., Burns, I., Rizkallah, P. J., Reid, K. B. M., and Greenhough, T. J. (2003) High-resolution structural insights into ligand binding and immune cell recognition by human lung surfactant protein D. *J. Mol. Biol. 331*, 509–523.
12. Crouch, E., McDonald, B., Smith, K., Cafarella, T., Seaton, B., and Head, J. (2006) Contributions of phenylalanine 335 to ligand recognition by human surfactant protein D. *J. Biol. Chem. 281*, 18008–18014.
13. Crouch, E., McDonald, B., Smith, K., Roberts, M., Mealy, T., Seaton, B., and Head, J. (2007) Critical role of arg/lys343 in the species-dependent recognition of phosphatidylinositol by pulmonary surfactant protein D. *Biochemistry 46*, 5160–5169.
14. Clark, H., and Reid, K. B. (2002) Structural requirements for SP-D function in vitro and in vivo: therapeutic potential of recombinant SP-D. *Immunobiology 205*, 619–631.
15. Garcia-Verdugo, I., Canadas, O., Taneva, S. G., Keough, K. M. W., and Casals, C. (2007) Surfactant protein A forms extensive lattice-like structures on 1,2-dipalmitoylphosphatidylcholine/rough-lipopolysaccharide-mixed monolayers. *Biophys. J. 93*, 3529–3540.
16. Gidalevitz, D., Ishitsuka, Y., Muresan, A. S., Konovalov, O., Waring, A. J., Lehrer, R. I., and Lee, K. Y. C. (2003) Interaction of antimicrobial peptide protegrin with biomembranes. *Proc. Natl. Acad. Sci. U.S.A. 100*, 6302–6307.
17. Roes, S., Seydel, U., and Gutsmann, T. (2005) Probing the properties of lipopolysaccharide monolayers and their interaction with the antimicrobial peptide Polymyxin B by Atomic Force Microscopy. *Langmuir 21*, 6970–6978.
18. Neville, F., Hodges, C. S., Liu, C., Konovalov, O., and Gidalevitz, D. (2006) In situ characterization of lipid A interaction with antimicrobial peptides using surface X-ray scattering. *Biochim. Biophys. Acta 1758*, 232–240.
19. Flach, C. R., Brauner, J. W., Taylor, J. W., Baldwin, R. C., and Mendelsohn, R. (1994) External reflection FTIR of peptide monolayer films *in situ* at the air/water interface - experimental design, spectra-structure correlations, and effects of hydrogen-deuterium exchange. *Biophys. J. 67*, 402–410.
20. Pezolet, M., and Labrecque, J. (1995) Surface pressure modulation of the conformation of poly(L-lysine) bound to phospholipid monolayers. *Biophys. J. 68*, A213.
21. Gericke, A., Flach, C. R., and Mendelsohn, R. (1997) Structure and orientation of lung surfactant SP-C and L-α-dipalmitoylphosphatidylcholine in aqueous monolayers. *Biophys. J. 73*, 492–499.
22. Kerth, A., Erbe, A., Dathe, M., and Blume, A. (2004) Infrared reflection absorption spectroscopy of amphipathic model peptides at the air/water interface. *Biophys. J. 86*, 3750–3758.
23. Brauner, J. W., Dugan, C., and Mendelsohn, R. (2000) ^{13}C isotope labeling of hydrophobic peptides. Origin of the anomalous intensity distribution in the infrared Amide I spectral region of β-sheet structures. *J. Am. Chem. Soc. 122*, 677–683.
24. Brauner, J. W., Flach, C. R., and Mendelsohn, R. (2005) A quantitative reconstruction of the Amide I contour in the IR spectra of globular proteins: From structure to spectrum. *J. Am. Chem. Soc. 127*, 100–109.
25. Bryan, M. A., Brauner, J. W., Anderle, G., Flach, C. R., Brodsky, B., and Mendelsohn, R. (2007) FTIR studies of collagen model peptides: Complementary experimental and simulation approaches to conformation and unfolding. *J. Am. Chem. Soc. 129*, 7877–7884.
26. Kuzmin, V. L., and Michailov, A. V. (1981) Molecular theory of light reflection and applicability limits of the macroscopic approach. *Opt. Spectrosc. (USSR) 51*, 383–385.
27. Kuzmin, V. L., Romanov, V. P., and Michailov, A. V. (1992) Reflection of light at the boundary of liquid systems and structure of the surface layer: A review. *Opt. Spectrosc. 73, 1*, 26; translated from *Opt. Spektrosk.* (1992) 73, 3−47.
28. Brandenburg, K., and Seydel, U. (1988) Orientation measurements on membrane systems made from lipopolysaccharides and free lipid A by FT-IR spectroscopy. *Eur. Biophys. J. 16*, 83–94.
29. Snyder, S., Kim, D., and McIntosh, T. J. (1999) Lipopolysaccharide bilayer structure: Effect of chemotype, core mutations, divalent cations, and temperature. *Biochemistry 38*, 10758–10767.
30. Flach, C. R., Xu, Z., Bi, X., Brauner, J. W., and Mendelsohn, R. (2001) Improved IRRAS apparatus for studies of aqueous monolayer films: Determination of the orientation of each chain in a fatty-acid homologous Ceramide 2. *Appl. Spectrosc. 55*, 1060–1066.
31. Brauner, J. W., Flach, C. R., Xu, Z., Bi, X., Lewis, R. N. A. H., McElhaney, R. N., Gericke, A., and Mendelsohn, R. (2003) Quantitative functional group orientation in Langmuir films by infrared reflection-absorption spectroscopy: C═O groups on behenic acid methyl ester and *sn*2-^{13}C-DSPC. *J. Phys. Chem. B 107*, 7202–7211.
32. Becker, R. (1964) *Electromagnetic Fields and Interactions*; Vol. II, Blaisdell Publishing Company: New York.
33. Wilson, E. B., Decius, J. C., and Cross, P. C. (1955) *Molecular Vibrations. The Theory of Infrared and Raman Vibrational Spectra*; McGraw-Hill: New York.
34. Seelig, A. (1987) Local anesthetics and pressure: a comparison of dibucaine binding to lipid monolayers and bilayers. *Biochim. Biophys. Acta 899*, 196–204.
35. Giehl, A., Lemm, T., Bartelsen, O., Sandhoff, K., and Blume, A. (1999) Interaction of the GM2-activator protein with phospholipid-ganglioside bilayer membranes and with monolayers at the air-water interface. *Eur. J. Biochem. 261*, 650–658.
36. Bi, X., Taneva, S., Keough, K. M. W., Mendelsohn, R., and Flach, C. R. (2001) Thermal stability and DPPC/Ca^{2+} interactions of pulmonary surfactant SP-A from bulk phase and monolayer IR spectroscopy. *Biochemistry 40*, 13659–13669.

37. Lad, M. D., Birembaut, F., Frazier, R. A., and Green, R. J. (2005) Protein-lipid interactions at the air/water interface. *Phys. Chem. Chem. Phys. 7*, 3478–3485.
38. Taneva, S., Voelker, D. R., and Keough, K. M. W. (1997) Adsorption of pulmonary surfactant protein D to phospholipid monolayers at the air-water interface. *Biochemistry 36*, 8173–8179.
39. Wang, L., Cai, P., Galla, H.-J., He, H., Flach, C. R., and Mendelsohn, R. (2005) Monolayer−multilayer transitions in a lung surfactant model: IR reflection−absorption spectroscopy and atomic force microscopy. *Eur. Biophys. J. 34*, 243–254.

BI800626H